Indian Journal of Biochemistry & Biophysics
Vol. 59, June 2022, pp. 675-686

Tumor cell and microvessel densities during the growth of a brain tumor: A theoretical study

Dibyajyoti Boruah* & Arijit Sen

Department of Pathology, Armed Forces Medical College, Pune-411 040, Maharashtra, India

Received 15 February 2022; *revised 07 April 2022*

Mathematical model for the tumor growth incorporating energy supply and requirement, angiogenesis efficiency and effect of elasticity of adjacent normal tissue to understand tumor biology and predict saturation status is rare to find. This study is conducted to address these issues. We propose mathematical expressions to explain alterations of tumor cell density (n_T), microvessel density (MVD), and growth rate(r) during the development of brain tumors. We assume that n_T increases during the growth of the tumor due to the increase of external pressure from the initial cell density (n_{T0}); n_{T0} is same as the external normal tissue. The rate of increase in tumor cells (dN_T/dt) depends on the rate of energy available for the creation of new cells and the energy required for a single cell division(γ). Due to the increase of tumor cell density, hypoxia is developed, which up-regulates the secretion of vascular endothelial growth factor (VEGF) and new capillaries are generated. Therefore, the surface area density of capillaries (A_{cs}) in tumors increases. Hence, we consider that $A_{cs}(t) \propto n_T(t)$. A modified logistic equation is developed. Temporal variations of $n_T(t)$, $A_{cs}(t)$, r(t) and tumor cell population '$N_T(t)$' are examined. The expressions of saturated cell density(n_{TM}), saturated microvessel surface area density (A_{csM}) and tumor saturation time(T_s) are formulated. An important feature, tumor saturation factor 'f_{TS}' is determined. When $f_{TS}<1$, a tumor will saturate at T_s, and n_{TM} depends solely on f_{TS}.

Keywords: Angiogenesis efficiency, Energy requirement, Saturated cell density, Saturated tumor cell population, Stress inside the tumor, Tumor saturation factor

Increased mitotic activities, angiogenesis, complex biological progressions, and getting away from immune surveillance are involved in the growth of a tumor. An appropriate mathematical model of tumor growth is very important to utilize the clinical and experimental data in the study of disease prognosis and treatment response[1-7]. The efficacy of a newer treatment modality, prediction of the effectiveness of radiotherapy, and optimization of anti-cancer drugs in cancer treatment can be studied with help of mathematical models[8-10]. Theoretical models incorporating tumor cell diffusions with proliferations have been extensively used by many researchers to study the growth patterns in highly infiltrative brain tumors like gliomas[8,11-16]. Such models are found very useful for predicting the duration of survival of patients and the effectiveness of cancer treatment[8,12].

The tumor cell density was reported to increase with the growth of a tumor confined by the basement membrane and surrounded by normal host tissues[11]. Studies performed on cultured tumor cell lines had suggested that the tumor cell density played an important role in controlling metastasis, drug resistance, and survival of the tumor in an unfriendly environment[12,17]. Glucose metabolism rate in a unit volume of astrocytomas was found to increase with the tumor cell density[18]. Cell density, microvessel density, microvessel diameter, and microvessel surface area per unit volume were found much larger in primary Central Nervous System (CNS) tumors than the normal brain tissue; and these parameters exhibited positive correlations with the histological grades of tumors[19-21]. The theoretical approach to explain such alterations in tumors is very limited to find in literature[4]. To date, we are unable to find mathematical expressions to predict the variation of tumor cell density and microvessel density during the growth of a tumor.

A tumor cannot proliferate to a size larger than 1-2 mm^3 without an efficient microvascular system for the nutrient supply[22]. Again, normal tissues in the vicinity of a tumor apply mechanical pressure due to the tissue elasticity, which oppose the growth of a tumor[1,4].

*Correspondence:
E-mail: dibyajyotibh@yahoo.co.uk

A tumor obtains necessary energy from the microvascular network in form of nutrients and utilizes that energy to maintain its living condition, to create new cells and space within normal tissue. In a recent work, a modified logistic equation for the tumor growth rate considering residual energy for cell division estimated from the energy supply and requirement rate has been used to study tumor growth and saturation status[4]. In that model, parameters like, per capita energy requirement rate for tumor cell maintenance, the elasticity of hosting tissue, and energy required for a single cell division are introduced; however, tumor cell density(n_T) and capillary surface area density(A_{cs}) are considered as constants during the tumor growth[4]. The same model is used in our present study, considering the variation of n_T and A_{cs} with time. We consider that cell density and microvessel density of a tumor increase with its expansion. The tumor cell density is affected by external pressure exerted by the surrounding tissue; that external pressure increases with the increases of tumor volume. Temporal variation of n_T, A_{cs}, and tumor growth rate(r) are studied for different conditions using numerical analysis. Analytical equations for maximum possible tumor cell population (N_{TM}), maximum possible tumor cell density (n_{TM}), tumor saturation time (T_s), initial tumor growth rate(r_0), and tumor growth rate at saturation (r_s) are formulated; and condition for saturation of a tumor is determined. Though, the genetic and epigenetic changes and immune system responses play key roles in the formation and growth of a tumor; but these factors are not included in this study.

Materials and Methods

A solid tumor in the brain has a higher cell density and microvessel density with a larger capillary diameter than the normal brain[19-21]. In the present work, it is assumed that, at the initiation of a tumor, cell density 'n_T' is the same as the density of surrounding normal tissue 'n_{T0}' and increases with the tumor size due to the increase of external pressure. The capillary surface area density 'A_{cs}' is considered as proportional to 'n_T' and angiogenesis efficiency 'α_{an}' of a tumor. To study the temporal variation of n_T and A_{cs}, it is necessary to develop a tumor growth equation. In a recent work, Boruah has developed a logistic equation for the tumor growth rate incorporating the energy supply and energy requirement terms; where n_T and A_{cs} were considered as constants[4]. It was assumed that the rate of increase in tumor cells(dN_T/dt) at a time 't' depends on the rate of energy available for the creation of new cells 'E_g', the energy required for a single cell division 'γ', and death rate 'δ'; *i.e.* $dN_T/dt=(E_g/\gamma - \delta N_T)$. In that work, E_g was determined from the energy supply rate and energy requirement rate for maintenance and creation of space in tumors. In the present work, the model of tumor growth developed by Boruah is used[4], and a modified logistic equation is formed incorporating variable $n_T(t)$ and $A_{cs}(t)$. An analytical solution of the modified logistic equation has been performed. The tumor saturation time 'T_s' is estimated, and equations for saturated tumor cell density 'n_{TM}', saturated capillary surface area density 'A_{csM}', initial growth rate 'r_0', saturated growth rate 'r_s', and the maximum possible number of tumor cell 'N_{TM}' are formulated. Numerical solutions are performed to demonstrate the theoretical formulations using MATLAB software. Estimation of the new parameters introduced in this work is performed using information from published articles[4,19,22-30].

Theory

The equation for tumor cell density 'n_T' and capillary surface area density 'A_{cs}'

The growth of a tumor is affected by its surrounding tissue imposing pressure upon it[4]. A tumor has to restrict its volume to limit internal stress and hence the space available for a single tumor cell is reduced continuously with tumor size. Hence, tumor cell density 'n_T' increases during the growth. At the time of initiation of a tumor, n_T can be considered as same as the density of the normal cells (n_{T0}) of its surrounding tissue. The density of tumor cells at a time t can be expressed as:

$$n_T(t) = n_{T0} + \alpha_{pn0}.\Delta P \qquad (1a)$$

Where α_{pn0} is the coefficient for an increase in cell density in a unit increase of pressure (unit: $Pa^{-1}.mm^{-3}$). ΔP is the external pressure on the tumor by the surrounding normal tissue (unit: Pa); that will produce the same amount of stress inside the tumor. Adopting Boruah's work[4], $\Delta P(t)$ can be expressed in terms of elasticity of normal brain tissue, tumor cell density 'n_T', number of tumor cell 'N_T' and, the coefficient of decrease in volume of the normal brain due to elastic compression 'α_v', as follows:

$$\Delta P(t) = \frac{K_V \alpha_v N_T(t)}{n_T(t)} \qquad (1b)$$

where, K_v is the ratio of bulk modulus of elasticity of normal brain tissue (K) to the volume of the normal brain tissue (V_n), and mean value of K_v=833 Pa.mm^{-34}. With equations (1a) and (1b) we have:

$$n_T(t) = \frac{n_{T0}}{2}\left[1 + \left(1 + \ b\mathrm{N_T(t)}\right)^{\frac{1}{2}}\right] \ where\ b = \frac{4\alpha_{pn0}\alpha_v \mathrm{K_V}}{n_{T0}^2} \quad (1c)$$

Using this equation we can obtain the density of tumor cells at any tumor cell population 'N_T'.

Studies on cell lines suggest that higher cell density increases the level of hypoxia-induced factors and VEGF[31-35]. Up-regulation of VEGF due to hypoxia is responsible for the creation of new capillaries in tumors[33-35]. Again, it was observed that capillary surface area density 'A_{cs}' showed strong positive correlations with the cell density[19]. Hence, in our work we assumed that A_{cs} is proportional to n_T; *i.e.*

$$\mathrm{A_{cs}(t)} = \alpha_{\mathrm{an}} n_T(t) = \frac{\alpha_{\mathrm{an}} n_{T0}}{2}\left[1 + \left(1 + \ b\mathrm{N_T(t)}\right)^{\frac{1}{2}}\right] \quad (1d)$$

where α_{an} is defined as the angiogenesis efficiency of a tumor (unit: mm^2) and is considered as a constant for a particular tumor.

The total microvessel surface area in the tumor 'A_{Tcs}' at a time can be estimated to from the tumor volume 'V_T' and A_{cs} as follows:

$$\mathrm{A_{Tcs}}(t) = \mathrm{V_T(t)A_{cs}(t)} = \frac{\mathrm{N_T(t)A_{cs}(t)}}{\mathrm{n_T(t)}} = \mathrm{N_T(t)}\alpha_{\mathrm{an}} \quad (1e)$$

The microvessel density 'MVD' (unit: mm^{-2}) can be evaluated from the mean capillary diameter 'd' and 'A_{cs}' as follows:

$$\mathrm{MVD} = \frac{\mathrm{A_{cs}}}{\mathrm{d}.\pi} \quad (1f)$$

Modified logistic equation and tumor saturation

A_{cs} and n_T in a tumor can be estimated at any time when $N_T(t)$ is known. $N_T(t)$ can be predicted from the solution of the tumor growth equation. The logistic equation for the tumor growth rate incorporating the energy availability rate for growth and energy required for a single cell division is given by:

$$\frac{\mathrm{dN_T}}{\mathrm{dt}} = \frac{\alpha_{sr}\alpha_{s0}A_{cs}\mathrm{N_T}}{\gamma n_T}\left(1 - \frac{\alpha_r n_T}{\alpha_{sr}\alpha_{s0}A_{cs}} - \frac{\alpha_{ps}\alpha_v K_v}{\alpha_{sr}\alpha_{s0}A_{cs}}\frac{\mathrm{N_T}}{n_T} - \frac{\gamma n_T \delta}{\alpha_{sr}\alpha_{s0}A_{cs}}\right) \quad (2a)$$

Using expressions for $n_T(t)$ and $A_{cs}(t)$ in the above equation from (1c) and (1d), respectively, we have:

$$\frac{\mathrm{dN_T}}{\mathrm{dt}} = \frac{\mathrm{N_T}}{\gamma}\left(\alpha_{sr}\alpha_{s0}\alpha_{an} - \alpha_r - \gamma\delta - \frac{4\alpha_{ps}\alpha_v K_v}{\mathrm{n_{T0}^2}}\frac{\mathrm{N_T}}{\left(1 + (1 + \ b\mathrm{N_T})^{\frac{1}{2}}\right)^2}\right) \quad (2b)$$

where,

γ is the energy required for a single cell division (unit: J).

α_{sr} is the relative permeability factor of the microvessel.

α_{s0} is the average rate of energy generated from the flux of nutrients passed through the unit capillary surface area in normal brain tissue (unit: W.mm^{-2}).

α_{an} is the angiogenesis efficiency of a tumor (unit: mm^2).

($\alpha_{sr}\alpha_{s0}\alpha_{an}$) represents the rate of microvascular energy supply to each tumor cell (unit: W/cell).

α_r is the rate of energy requirement for regular maintenance of a single cell (unit: W/cell).

δ is the death rate (unit: s^{-1}).

($\gamma\delta$) represents the per capita rate of energy expenditure due to death of tumor cells (unit: W/cell).

α_{ps} is the rate of energy required for the expansion of the unit volume of a tumor to overcome unit external pressure; (unit: W.mm^{-3}Pa^{-1}).

α_v is the coefficient of decrease in volume of the normal brain due to elastic compression. (1- α_v) represents the degeneration of normal brain tissue due to tumor expansion in terms of tumor volume.

The last term, $\left(4\alpha_{ps}\alpha_v K_v \mathrm{N_T}/\left(n_{T0}\left(1 + (1 + \ b\mathrm{N_T})^{\frac{1}{2}}\right)\right)^2\right)$, represents the per capita rate of energy expenditure due to the expansion of tumor (unit: W/cell).

The equation (2b) can be expressed as:

$$\frac{\mathrm{dN_T}}{\mathrm{dt}} = \frac{\mathrm{N_T}}{\gamma}\left(\mathrm{c_1} - \frac{\mathrm{c_2 N_T}}{\left(1 + (1 + \ b\mathrm{N_T})^{\frac{1}{2}}\right)^2}\right) \quad (2c)$$

where,

$b = \frac{4\alpha_{pn0}\alpha_v \mathrm{K_V}}{n_{T0}^2}$ (dimension less)

$c_1 = \alpha_{sr}\alpha_{s0}\alpha_{an} - \alpha_r - \gamma\delta$ (unit: W)

$\mathrm{c_2} = \frac{4\alpha_{ps}\alpha_v K_v}{\mathrm{n_{T0}^2}} = \frac{b\alpha_{ps}}{\alpha_{pn0}}$ (unit: W)

Equation (2c) is the modified logistic equation for tumor growth with variable n_T and A_{cs} and its solution could be obtained using boundary conditions as $N_T(t=0)=N_{T0}$ at t=0, and $N_T(t)=N_T$ at t=t, as follows:

$$t = \frac{2\gamma}{c_3(c_4+1)} log\left[\left\{\frac{(1+bN_T)^{\frac{1}{2}}-1}{(1+bN_{T0})^{\frac{1}{2}}-1}\right\}\left\{\frac{(1+bN_T)^{\frac{1}{2}}+c_4}{(1+bN_{T0})^{\frac{1}{2}}+c_4}\right\}^{c_4}\right] \quad (2d)$$

where,

$$c_3 = \frac{c_1 b - c_2}{b} = \alpha_{sr}\alpha_{s0}\alpha_{an} - \alpha_r - \gamma\delta - \frac{4\alpha_{ps}\alpha_v K_v}{b n_{T0}^2}$$

(unit: W)

$$c_4 = \frac{c_1 b + c_2}{c_1 b - c_2} = \frac{\left(\alpha_{sr}\alpha_{s0}\alpha_{an} b - \alpha_r b - \gamma\delta b + \frac{4\alpha_{ps}\alpha_v K_v}{n_{T0}^2}\right)}{\left(\alpha_{sr}\alpha_{s0}\alpha_{an} b - \alpha_r b - \gamma\delta b - \frac{4\alpha_{ps}\alpha_v K_v}{n_{T0}^2}\right)}$$

(dimension less)

A tumor will grow continuously with time when the rate of increase of cells is never diminishing to zero. In this work, we have found that the saturation of a tumor depends on a composite parameter (bc_1/c_2), which is named as tumor saturation factor 'f_{TS}'.

$$f_{TS} = b\frac{c_1}{c_2} = \frac{\alpha_{pn0}}{\alpha_{ps}}(\alpha_{sr}\alpha_{s0}\alpha_{an} - \alpha_r - \gamma\delta) \quad (2e)$$

When $f_{TS}<1$, the tumor will reach its saturation at a certain time, otherwise it will grow continuously. The following condition must be followed by a tumor for saturation:

$$\alpha_{sr}\alpha_{s0}\alpha_{an} < \left(\frac{\alpha_{ps}}{\alpha_{pn0}} + \alpha_r + \gamma\delta\right) \quad (2f)$$

Hence, the size of a tumor will be restricted to a certain limit, when α_{sr}, α_{an}, α_{pn0} are smaller and α_{ps}, α_r, γ, and δ are larger. When $f_{TS}<1$, saturated cell density 'n_{TM}', saturated capillary surface area density 'A_{csM}', and maximum possible capillary surface area within the tumor 'A_{TcsM}' could be predicted from the value of maximum possible cell population 'N_{TM}' of the tumor attained at saturation time. N_{TM} can be estimated by considering $\frac{dN_T}{dt} = 0$. Using this condition and putting $N_T = N_{TM}$, in equation (2b), we obtain:

$$N_{TM} = \frac{4f_{TS}}{b(1-f_{TS})^2} = \frac{n_{T0}^2(\alpha_{sr}\alpha_{s0}\alpha_{an} - \alpha_r - \gamma\delta)}{\alpha_{ps}\alpha_v K_v\left(1 - \frac{\alpha_{pn0}}{\alpha_{ps}}(\alpha_{sr}\alpha_{s0}\alpha_{an} - \alpha_r - \gamma\delta)\right)^2}, f_{TS} < 1 \quad (3a)$$

$$n_{TM} = \frac{n_{T0}}{2}\left(1 + (1+bN_{TM})^{\frac{1}{2}}\right) = \frac{n_{T0}}{(1-f_{TS})} = \frac{n_{T0}}{\left(1 - \frac{\alpha_{pn0}}{\alpha_{ps}}(\alpha_{sr}\alpha_{s0}\alpha_{an} - \alpha_r - \gamma\delta)\right)}, f_{TS} < 1 \quad (3b)$$

$$A_{csM} = \alpha_{an} n_{TM} \quad (3c)$$

$$A_{TcsM} = \alpha_{an} N_{TM} \quad (3d)$$

The maximum possible volume of the tumor 'V_{TM}' can be expressed as:

$$V_{TM} = \frac{N_{TM}}{n_{TM}} = \frac{4f_{TS}}{n_{T0}b(1-f_{TS})} = \frac{n_{T0}(\alpha_{sr}\alpha_{s0}\alpha_{an} - \alpha_r - \gamma\delta)}{\alpha_{ps}\alpha_v K_v\left(1 - \frac{\alpha_{pn0}}{\alpha_{ps}}(\alpha_{sr}\alpha_{s0}\alpha_{an} - \alpha_r - \gamma\delta)\right)}, f_{TS} < 1 \quad (3e)$$

Saturation time, T_s of a tumor can be obtained from equation(2d) using the value of N_{TM}. The equation (2d) gives an undetermined value for the estimation of T_s when we put $N_T = N_{TM}$. Hence the time required for a tumor to attain its 99.9% of the maximum population from the initial number of cell $N_{T0}=1$, is considered as T_s and obtained by putting $N_T = 0.999N_{TM} = N_s$ in equation (2c) as follows:

$$T_s = \frac{2\gamma}{c_3(c_4+1)} log\left[\left\{\frac{(1+bN_s)^{\frac{1}{2}}-1}{(1+b)^{\frac{1}{2}}-1}\right\}\left\{\frac{(1+bN_s)^{\frac{1}{2}}+c_4}{(1+b)^{\frac{1}{2}}+c_4}\right\}^{c_4}\right], f_{TS} < 1 \quad (3f)$$

The growth rate of tumor 'r' can be defined from the growth equation (2c) by rearranging in the form of its canonical equation, $\frac{dN_T}{dt} = rN_T\left(1 - \frac{N_T}{N_{TM}}\right)$ as follows:

$$r = \left(c_1 - \frac{c_2 N_T}{\left(1 + (1 + bN_T)^{\frac{1}{2}}\right)^2}\right) \Big/ \gamma\left(1 - \frac{N_T}{N_{TM}}\right), N_{TM} = \frac{4c_1}{c_2(1-f_{TS})^2} \text{ for } f_{TS} < 1 \quad (4a)$$

$$= \infty \text{ or } f_{TS} > 1$$

The growth rate 'r' of a tumor varies with time since N_T is a function of time. The growth rate at the initiation of a tumor (r_0) can be estimated from equation (4a). At t=0, $N_T=1$ and hence $bN_T<<1$, $N_{TM}>>N_T$, therefore:

$$r_0 = r(t=0, N_T = 1) = \frac{\left(c_1 - \frac{c_2}{4}\right)}{\gamma} = \frac{1}{\gamma}(\alpha_{sr}\alpha_{s0}\alpha_{an} - \alpha_r - \frac{\alpha_{ps}\alpha_v K_v}{n_{T0}^2}) - \delta \quad (4b)$$

The initial growth rate when death rate $\delta=0$:

$$r_{0(\delta=0)} = \frac{1}{\gamma}(\alpha_{sr}\alpha_{s0}\alpha_{an} - \alpha_r - \frac{\alpha_{ps}\alpha_v K_v}{n_{T0}^2}) \quad (4c)$$

A tumor cannot grow when the initial growth rate is equal to the death rate. The growth rate at the saturation of a tumor 'r_s' can be determined for limiting value $N_T \rightarrow N_{TM}$ when $f_{TS}<1$. Putting $N_T=0.999N_{TM}=N_s$ in equation (4a):

$$r_s = \left(c_1 - \frac{c_2 N_s}{\left(1+(1+\ bN_s)^{\frac{1}{2}}\right)^2} \right) \Big/ \gamma \left(1 - \frac{N_s}{N_{TM}}\right), \text{for } f_{TS} < 1 \qquad (4d)$$

Estimation of the parameters

Prediction of n_T, A_{cs}, A_{Tcs}, r, N_T, and tumor volume 'V_T' at any time of growth is an important aspect for the assessment of brain tumors in different conditions. The numerical solution of the equation(2c) provides the temporal profile of N_T, and hence n_T, A_{cs}, A_{Tcs}, and 'r' of a tumor could be estimated. Equations (3a) to (3f) provide N_{TM}, n_{TM}, A_{csM}, A_{TcsM}, V_{TM} and T_s, respectively. To apply these equations for the brain tumors, the suitable value and range of the coefficients used in the equations have to be estimated. In the numerical studies presented in this work, the range of n_{T0}, α_{sr}, α_{s0}, α_v, K_v, α_{ps}, γ and δ are kept the same as estimated by Boruah in his work, where n_T and A_{cs} have been considered as constants during the growth for a tumor[4]. α_{pn0} and α_{an} will be estimated using equations (1a) and (1d) at the saturation of tumor as follows:

$$\alpha_{pn0} = \frac{n_{TM} - n_{T0}}{\Delta P_M} \qquad (5a)$$

$$\alpha_{an} = \frac{A_{csM}}{n_{TM}} \qquad (5b)$$

where, ΔP_M is the maximum stress inside the tumor that attained at the tumor saturation, and considered as $\Delta P_M=2x10^3$Pa, because it is comparable to the average pressure inside a capillary measured at the heart level in human[4]. If the stress is more that 2×10^3 Pa, blood cannot flow though the capillary in tumors. n_{T0} is the cell density of a tumor at the beginning, which is considered same as the cell density of normal brain. Using histological sections of normal brain tissue obtained from autopsy cases, and applying images morphometry on the microscopic images, n_{T0} was estimated[4,19]. n_{TM} is the maximum cell density and A_{csM} is the maximum capillary surface area density of a brain tumor attained at its saturation. The histological sections of brain tumor tissues stained by CD34 immuno-hitsochemical (IHC) marker were used to highlight the capillaries[19]. The total length of boundary of capillaries per unit area of a tissue section can be estimated using image morphometric techniques. The capillary can be considered as a cylindrical structure. Total length of boundary of capillaries per unit area found in plane section, can be considered as the total capillary surface area per unit volume of tissue (A_{cs}) in a 3D scenario. A_{cs} was calculated from the mean diameter of capillaries (d) and microvascular density (MVD) using the relation, $A_{cs} = \pi.d.MVD$[4,19]. In most of the cases of brain tumors, histo-pathological examination is performed only after surgical removal of the tumor. At the time of removal, a tumor can be considered to reach its saturation. Hence, we consider morphometrically measured cell density for tumors as n_{TM} and capillary surface area density as A_{csM} for estimation of α_{pn0} and α_{an}. Mean cell density and capillary surface area density with standard deviation reported for 10 normal brain tissue were: $n_{T0}=3.7 \times 10^4$ mm^{-3} (range: 2.5×10^4 - 4.6×10^4) and $A_{cs}=3.90$ mm^{-1} (range: 2.60-4.80)[19]. Mean n_{TM} and A_{csM} with standard deviation reported for 30 gliomas were: (I) $n_{TM}=1.99 \times 10^5 \pm 1.42 \times 10^5$ mm^{-3} (0.56×10^5 - 4.23×10^5) and $A_{csM}=7.06 \pm 1.27$ mm^{-1} (5.67-10.19) in low grades; and (ii) $n_{TM}= 3.17 \times 10^5 \pm 0.98 \times 10^5$ mm^{-3} ($1.85x10^5$ - 5.07×10^5) and $A_{csM}=10.86 \pm 2.57$ mm^{-1} (6.90-15.73) in high grades[19]. α_{pn0} is estimated for a tumor using these values of n_{TM}, n_{T0} and ΔP_M; and α_{an} is estimated from the ratio of A_{csM} and n_{TM}. For the normal brain tissue, n_T and A_{cs} can be considered as invariant with time, hence $n_{TM}= n_{T0}$ and $A_{csM}=A_{cs}$. The mean value with standard deviation(SD) and range of α_{pn0} and α_{an} estimated from the data of the reported cases[19], using equations (5a) & (5b) are: (i) In normal brain: $\alpha_{pn0}=0$ & $\alpha_{an}=10.65 \times 10^{-5} \pm 1.58 \times 10^{-5}$ mm^2 (8.59×10^{-5} -13.38×10^{-5}); (ii) In low grade gliomas: $\alpha_{pn0}=81 \pm 71$ Pa^{-1} mm^{-3} (9-193) & $\alpha_{an} =5.16 \times 10^{-5} \pm 3.23 \times 10^{-5}$ mm^2 (1.36×10^{-5}-11.95×10^{-5}); (iii) in high grade gliomas: $\alpha_{pn0}=140 \pm 49$ Pa^{-1} mm^{-3} (74-235) & $\alpha_{an}=3.75 \times 10^{-5} \pm 1.41 \times 10^{-5}$ mm^2 (1.73×10^{-5}-5.73×10^{-5}).

Results

In this work, we consider that, $\alpha_{sr}=1$, $\alpha_{s0}=3.23 \times 10^{-6}$ W.mm^{-2}, $n_{T0}=3.7 \times 10^4$ mm^{-3}, $K_v=833$ Pa.mm^{-3} and $\alpha_v=1.3 \times 10^{-4}$, and are kept unchanged throughout numerical studies. Variations on N_T, (dN_T/dt), n_T, A_{cs}, r with time, and saturated values N_{TM}, n_{TM}, A_{csM}, T_s, r_s, and initial growth rate 'r_0' of tumors with f_{TS}, δ, α_r, α_{ps}, α_n, α_{pn0} and γ, are studied numerically. Temporal variation of number of tumor cell 'N_T' obtained from

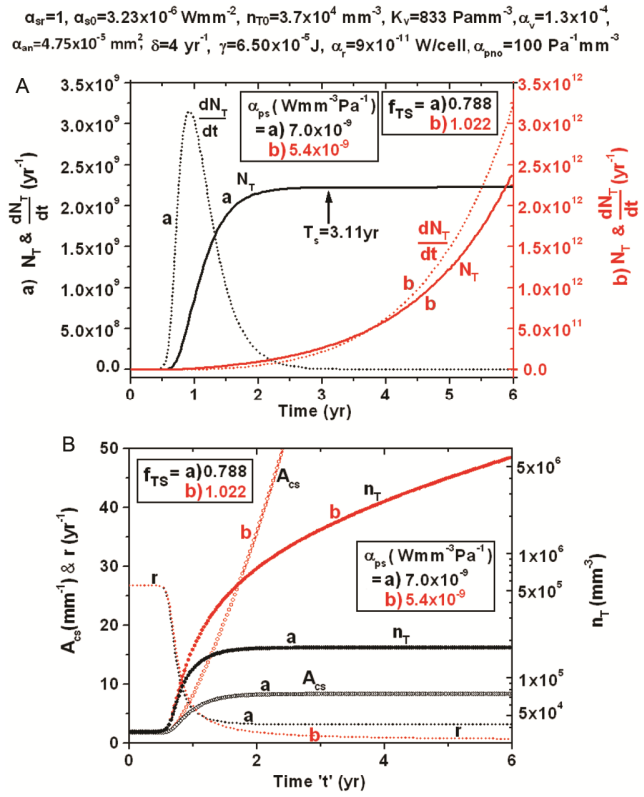

Fig. 1 — (A) Temporal variation of number of tumor cell 'N_T' obtained from numerical solutions of equation (2c) for two values of tumor saturation factor, f_{TS}= a) 0.788 & b) 1.022. The dotted curves represent the rate of change of tumor cell population (dN_T/dt) with time't', obtained by differentiating the respective graphs of N_T.; and (B) Temporal variation of the tumor cell density 'n_T', and capillary surface area density 'A_{cs}', obtained from numerical solutions of equations (1c), (1d) and (2c), and growth rate 'r' obtained from equation (4a) for the two f_{TS}. The two values of f_{TS} are obtained for α_{ps}= a) 7.0×10^{-9} $Wmm^{-3}Pa^{-1}$ & b) 5.4×10^{-9} Wmm^{-3} Pa^{-1}. The values of α_{sr}, α_{s0}, n_{T0}, K_v, α_v, α_{an}, δ, γ, α_r and α_{pn0}, used in the estimation of N_T, (dN_T/dt), n_T, A_{cs} and 'r' in the graphs are kept constant and presented in the top

numerical solutions of equation (2c) for two values of f_{TS}=a) 0.788 & b) 1.022, is presented in (Fig. 1A). The rate of change of tumor cell population (dN_T/dt) with time 't' obtained by differentiating the respective graphs of N_T for each f_{TS} is presented by dotted curves in the figure. The two values of f_{TS} are obtained for α_{ps}=a) 7.0×10^{-9} Wmm^{-3} Pa^{-1} & b)5.4×10^{-9} Wmm^{-3} Pa^{-1}, and all other parameters kept as: α_{an}=4.75×10^{-5} mm^2, δ=4 yr^{-1}, γ=6.50×10^{-5}J, α_r=9×10^{-11} W/cell, α_{pn0}=100 Pa^{-1} mm^{-3} and also shown in the top of the figure. Temporal variation 'n_T' and 'A_{cs}' obtained from numerical solutions of equations (1c), (1d), and (2c), and growth rate 'r' obtained from equation (4a) for the two f_{TS} are presented in (Fig. 1B). When f_{TS}<1 for a tumor, as shown in the graphs 'a' in (Fig. 1A & B); the tumor reaches its saturation; N_T, n_T and A_{cs} increase nonlinearly with time and attain there maximum value at saturation time T_s. The plot of (dN_T/dt) with time has exhibited right-skewed Gaussian pattern; a similar plot could be observed for (dn_T/dt) with time. The growth rate 'r' decreases from its maximum initial value(r_0) with time and reaches the minimum value(r_s) at tumor saturation. When f_{TS}>1 for a tumor, as shown in the graphs of 'b', N_T, (dN_T/dt), n_T and A_{cs} never get saturated and increase indefinitely. 'r' decreases continuously and never reaches to a fixed minimum value for f_{TS}>1.

Temporal variation of tumor cell density 'n_T' obtained from numerical solutions of equations (1c) and (2c) and growth rate 'r' using equation (4a) for six values of death rate, δ [= a) 0, b) 2 yr^{-1}, c) 5 yr^{-1}, d) 10 yr^{-1}, e) 20 yr^{-1}& f) 30.79 yr^{-1} = $r_{0(\delta=0)}$], keeping other parameters unchanged, are presented in the (Fig. 2A). n_T increases with time and reaches the maximum value(n_{TM}) and 'r' decreases with time and reaches the minimum value(r_s) at tumor saturation. With the increase of δ, n_{TM} and initial growth rate 'r_0' decrease and r_s increases. If δ is equal to the initial growth rate of a tumor, then the tumor cannot grow, as seen in the graph 'f'. Variations of tumor saturation factor 'f_{TS}' and saturated tumor cell population 'N_{TM}' with death rate 'δ' for two values of α_{pn0} [= a)60 Pa^{-1} mm^{-3} & b) 100 Pa^{-1} mm^{-3}], when other parameters are kept constant, are presented in (Fig. 2B). f_{TS} decreases linearly with δ. For a higher value of α_{pn0}, f_{TS} is larger at a particular δ, and the rate of decrease of f_{TS} with δ is higher. N_{TM} decreases nonlinearly with δ, and it is larger for higher values of α_{pn0} at a particular δ. Variation of n_{TM}, r_0, r_s, and saturation time 'T_s' with δ for two values of α_{pn0} are presented in the (Fig. 2C). n_{TM} decreases with the increase of δ, and n_{TM} at a particular δ is higher for higher α_{pn0}. r_0 decreases linearly with δ, and it does not change with α_{pn0}. r_s increases to a maximum and then decreases with δ. r_s is larger for a smaller α_{pn0} at a particular δ. T_s decreases slowly at first and then increases with δ for larger α_{pn0}; whereas, T_s increases with δ for smaller α_{pn0}; In both cases, the rate of increases of T_s with δ is higher at larger δ.

Variation of f_{TS} and N_{TM} with rate of energy requirement for maintenance per cell 'α_r' for two values of α_{ps} [=a) 6.50 WPa^{-1} mm^{-3} & b) 5.75 WPa^{-1} mm^{-3}] are presented in the (Fig. 2D). f_{TS} shows linear

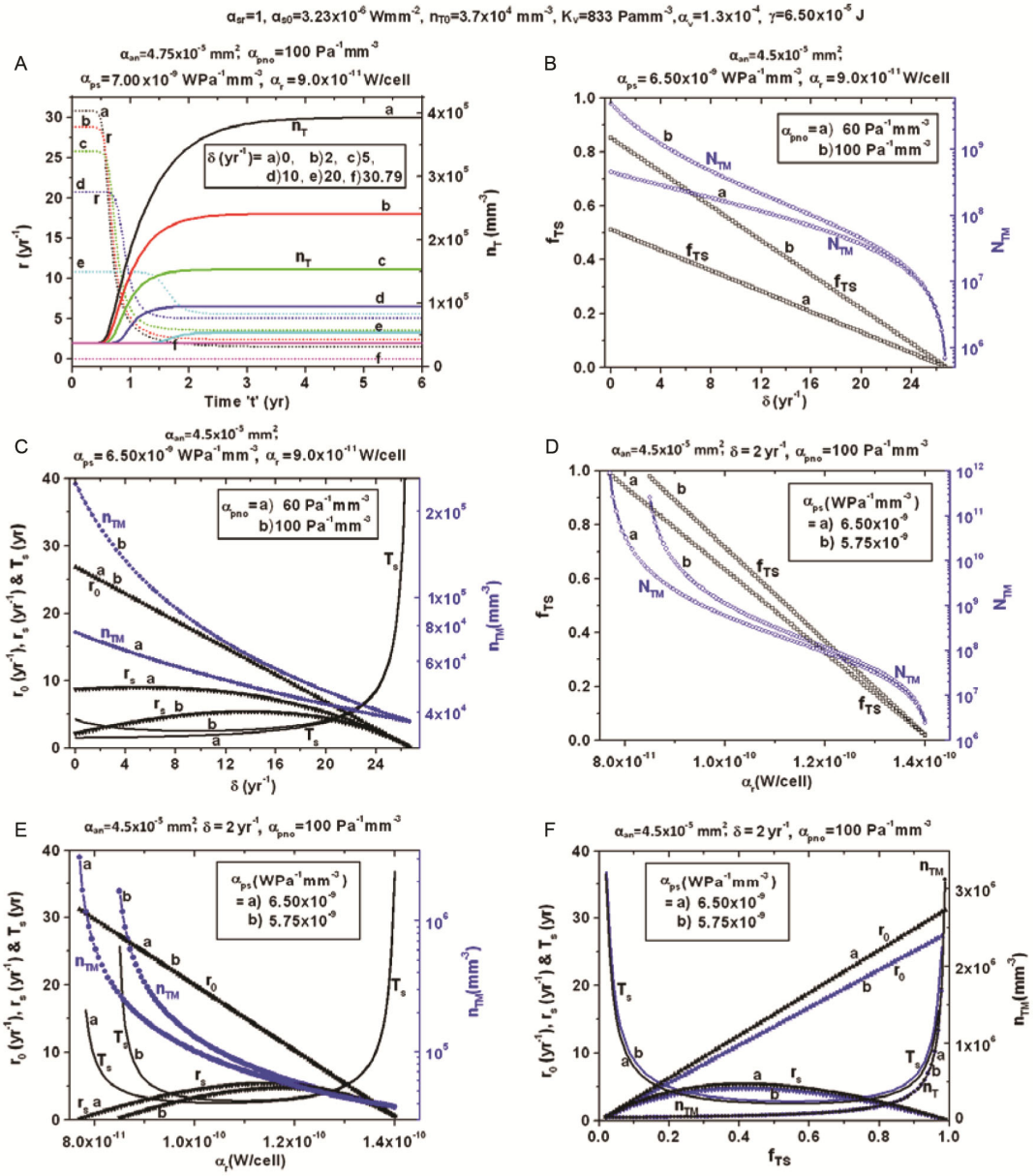

Fig. 2 —(A) Temporal variation of the tumor cell density 'n_T' obtained from numerical solutions of equations(1c) & (2c), and growth rate 'r' using equation (4a) for six values of death rate, δ = a) 0, b) 2 yr^{-1}, c) 5 yr^{-1}, d)=10 yr^{-1}, e) 20 yr^{-1} & f) 30.79 yr^{-1}=r_0(δ=0); (B) Variation of tumor saturation factor 'f_{TS}' and saturated tumor cell population 'N_{TM}' with death rate 'δ' for two values of α_{pn0}=a) 60 Pa^{-1} mm^{-3} & b) 100 Pa^{-1} mm^{-3}; (C) Variation of saturated tumor cell density 'n_{TM}', initial growth rate 'r_0', saturated growth rate 'r_s', and saturation time 'T_s' with 'δ' for two values of α_{pn0}; (D) Variation of 'f_{TS}' and 'N_{TM}' with rate of energy requirement for maintenance per cell 'α_r' for two values of α_{ps}= a) 6.50 WPa^{-1} mm^{-3} & b) 5.75 WPa^{-1} mm^{-3}; (E) Variation of n_{TM}, r_0, r_s, and T_s with α_r for two values of α_{ps}; and (F) Variation of n_{TM}, r_0, r_s, and T_s with tumor saturation factor 'f_{TS}' for two values of α_{ps}. The values of α_{sr}, α_{s0}, n_{T0}, K_v, α_v, and γ used in the estimation of the parameters for the graphs are kept fixed in all figures (A) to (F) as shown in the top. The values of α_{an}, δ, α_r, α_{ps} and α_{pn0} used for the graphs are presented in each figure, except the variables

decrease and N_{TM} shows nonlinear decrease with α_r, when other parameters are kept unchanged. (Fig. 2E) shows the variations of n_{TM}, r_0, r_s, and T_s with α_r for two values of α_{ps}. n_{TM} decreases nonlinearly and r_0 decreases linearly with α_r. r_s increases to a maximum value and then decreases with α_r. T_s decreases to a minimum and then increases with α_r. At a particular α_r; n_T and T_s are smaller and r_s is larger for larger α_{ps}; whereas, r_0 does not change with α_{ps}. Dependencies of n_{TM}, r_0, r_s, and T_s with α_{ps} are decreased with the

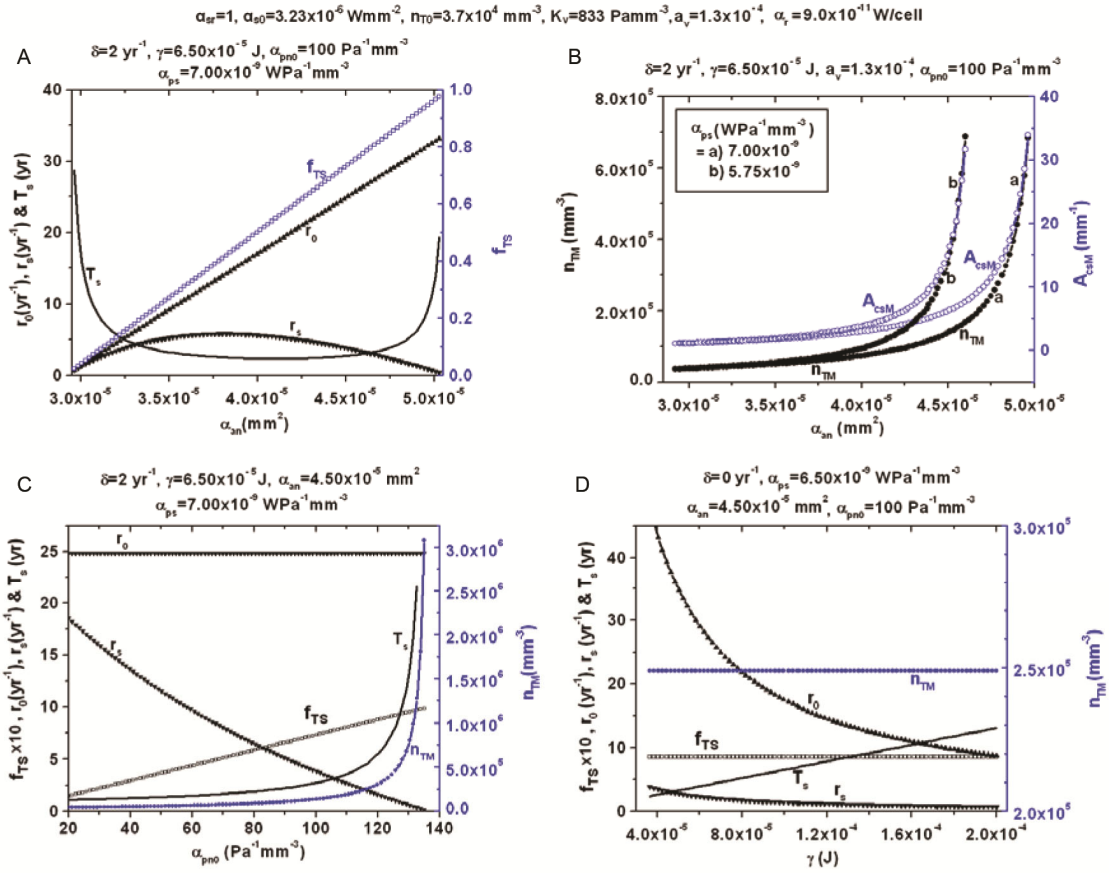

Fig. 3 — (A) Variation of f_{TS}, r_0, r_s, and T_s with the angiogenesis efficiency 'α_{an}'; (B) Variation of n_{TM}, and saturated capillary surface area density 'A_{csM}' with α_{an} for two values of α_{ps}=a) 7.00×10^{-9} WPa^{-1} mm^{-3} and b) 5.75×10^{-9} WPa^{-1} mm^{-3}; (C) Variation of n_{TM}, f_{TS}, r_0, r_s, and T_s with α_{pn0}; and (D) Variation of n_{TM}, f_{TS}, r_0, r_s, and T_s with the energy required for a single cell division 'γ'. The values of α_{sr}, α_{s0}, n_{T0}, K_v and α_v, α_r used in the estimation of the parameters for the graphs are kept fixed in all figures (A) to (D) as shown in the top. The values of α_{an}, δ, γ, α_{ps} and α_{pn0} used for the graphs are presented in each figure, except variables

increase of α_r. Variation of n_{TM}, r_0, r_s, and T_s with tumor saturation factor 'f_{TS}' for two values of α_{ps} are presented in (Fig. 2F). n_{TM} and r_0 increase with f_{TS}. r_s increases first to a maximum value and then decreases with f_{TS}. At a particular f_{TS}, r_0 is larger for higher α_{ps}; r_s and T_s are almost unchanged with α_{ps}, whereas, n_{TM} depends only on f_{TS}.

Variation of f_{TS}, r_0, r_s, and T_s with the angiogenesis efficiency 'α_{an}' are presented in (Fig. 3A). f_{TS} and r_0 increase linearly with α_{an}. r_s increases at first to a maximum value then decreases with α_{an}. T_s decreases to minimum value then increases with α_{an}. Variation of n_{TM}, and saturated capillary surface area density 'A_{csM}' with α_{an} for two values of α_{ps} [= a) 7.00×10^{-9} WPa^{-1} mm^{-3} and b) 5.75×10^{-9} WPa^{-1} mm^{-3}] are presented in the (Fig. 3B). n_{TM} and A_{csM} increase exponentially with α_{an}. At a particular α_{an}, n_{TM} and A_{csM} are larger for smaller α_{ps}.

Variation of n_{TM}, f_{TS}, r_0, r_s, and T_s with α_{pn0} are shown in (Fig. 3C). Nonlinear increases of n_{TM} and T_s with α_{pn0}, and linear increases of f_{TS} with α_{pn0} are observed. r_0 remains unchanged and r_s decreases with α_{pn0}. (Fig. 3D) shows variations of n_{TM}, f_{TS}, r_0, r_s, and T_s with the energy required for a single cell division 'γ' for δ=0. n_{TM} and f_{TS} remain unchanged with γ; r_0 and r_s decrease and T_s increases with γ. When δ>0, variations of f_{TS}, n_{TM}, r_0, r_s, and T_s with γ, would show similar variations with δ as shown in (Fig. 2B & C).

Discussion

Malignancy is a genetic disorder that involves active transforms in the genome and has distinctive characteristics of the tumor cells, like, unbounded multiplicative potential, continual angiogenesis, prevention of apoptosis, non-sensitive to anti-growth signals, tissue invasion and metastasis, avoidance of

immune destruction, and reprogramming of energy metabolism[36-37]. Immune responses from hosting tissues, intrinsic properties of tumor cells and tumor location influence the growth of malignant tumors[37-38]. In the case of normal cells, the replication is controlled by the extracellular stimulus unlike in cancers. To carry out replication of a cell, it must duplicate its genome, proteins, and lipids and arrange these constituents into daughter cells, which require a sufficient amount of energy. Demand for energy in a unit volume of cancerous tumors is more since the rate of cell division is much higher in tumors than the normal tissues. Hence, neoangiogenic vessels are found in brain tumors besides preexisting blood vessels in external tissues[39]. The growth of a malignant tumor is affected by the energy supply rate per unit volume, and energy required for maintenance and overcoming external pressure[4]. Due to the increased mitosis in brain tumors, the density of tumor cells increases, since tumor expansion is resisted by the elasticity of normal brain tissue. In such conditions, a tumor has to increase its microvessel density to meet the increased demand for nutrients. Hence, cell density and microvessel density in brain tumors is greater than the external normal tissue[19]. In the present work, we have developed a theoretical model to explain the temporal variation as well as saturated values of tumor cell population, size, cell density and microvessel density, which could be applied in brain tumors. In our model, time-dependent n_T and A_{cs} have been incorporated into the logistic equation for the tumor growth rate considering energy requirement terms as reported by Boruah[4].

The stress inside the tumor increases with its enlargement, hence per capita rate of energy expenditure due to the expansion of tumor increases with tumor size. Therefore, resource limitation for tumor growth arises with time. We found that the tumor cell population, cell density, capillary surface area density and volume at saturation, initial growth rate, and saturated growth rate are manipulated by parameters: δ, α_{an}, α_{pn0}, α_{ps}, α_{sr}, α_r and γ. It is very challenging to determine the effects of these parameters on the growth of tumors using an experimental setup. An important factor that includes effects of all these parameters, tumor saturation factor 'f_{Ts}' is established in this study, which could be utilized to predict the saturation status of a tumor. A tumor will be saturated when $f_{TS}<1$, otherwise it will grow indefinitely as demonstrated in (Fig 1A & B). Since the indefinite growth of a tumor is difficult to justify, it is unlikely to get $f_{TS}\geq 1$ for a tumor. f_{TS} is larger for a tumor having larger n_{TM} and A_{csM}. The expected value of the tumor saturation factor of saturated tumors can be evaluated using relation, $f_{TS}=1-n_{T0}/n_{TM}$, obtained from equation (3b). Using data from Boruah *et al*[19], it is found that: (i) In low-grade gliomas, mean with SD and range of $f_{TS}= 0.70 \pm 0.19$ (0.35-0.91), and (ii) In high-grade gliomas, mean with range of $f_{TS}= 0.87 \pm 0.04$ (0.80-0.93). Hence, f_{TS} is larger for high-grade gliomas, and this set of gliomas follows the relation: $0.35 < \frac{\alpha_{pn0}}{\alpha_{ps}} \left(\alpha_{sr}\alpha_{s0}\alpha_{an} - \alpha_r - \gamma\delta\right) < 0.93$. Since, α_{s0} is a constant and α_{an} is found to decrease with the grade of gliomas, a higher grade gliomas or malignant tumor should have larger α_{sr} and/or smaller α_r, γ, δ and (α_{ps}/α_{pn0}).

In a tumor inside the brain, the parameters α_{pn0}, α_{ps}, α_{sr}, α_{an}, α_r, γ and δ should adjust themselves to make $f_{TS}<1$. These parameters of a tumor cannot take any arbitrary values; each parameter has either a lower or an upper limit for a set of parameters found in expression of f_{TS}. If tumors have to be saturated, α_{ps}, α_r and γ should have lower limits, and α_{pn0}, α_{sr} and α_{an} should have upper limits. Maximum possible tumor cell population 'N_{TM}', saturated tumor cell density 'n_{TM}' and capillary surface area density 'A_{csM}', and tumor saturation time 'T_s' are the important biological parameters for the prediction of the outcome of a patient having brain tumor. N_{TM}, n_{TM}, A_{csM} and T_s are nonlinear functions of the tumor parameters as depicted by the equations (3a), (3b), (3c) and (3f), respectively. Degrees of influence of the parameters, α_{pn0}, α_{ps}, α_{sr}, α_{an}, α_r ,γ, α_v and K_v on N_{TM}, n_{TM}, A_{csM} and T_s depend on their range. In the range of our numerical study, we observed that α_r is the most sensitive parameter, followed by α_{an}, α_{ps} and α_{pn0}. Such types of parameters were not defined previously in any experimental study. The parameter 'α_{an}', defined in this work is directly related to angiogenesis. Angiogenesis is considered as one of the prominent features in malignant brain tumors; and anti-angiogenesis therapy is widely used for cancer treatment[35]. The growth rate, N_{TM}, A_{csM} and n_{TM} of a tumor can be reduced greatly by enhancing the rate of energy requirement for regular maintenance of a single cell 'α_r'. A cell will be highly ordered when it has a large value of α_r. If some methods could be devised to enhance α_r of tumor cells, then, N_{TM}, n_{TM} and A_{csM} could be controlled to a safer limit. The concept of modulation of α_r may be applied to explain

positive effects of mindfulness meditation, yoga, and pranayama for oncology patients[40].

Our study suggests that $n_{TM,}$ as well as A_{csM}, are constant for a particular value of f_{TS}. N_{TM} and V_{TM} are inversely proportional to 'b' at a constant f_{TS}. If value of 'b' is smaller (*i.e.* α_{pn0}, α_v & K_v are small), the saturated volume of a tumor will be more for a particular n_{TM}. The human brain is composed of soft tissues having a range of shear modulus of elasticity 0.4–2.1 kPa and the bulk modulus of elasticity 1.0-2.7 GPa[28,41]. During the growth of a tumor, it has to compress, deform and degenerate the normal brain tissue to create space and expense energy in this process. The energy to create space for a tumor depends on the degeneration and elastic properties of the external normal tissue[4]. If normal external tissue has strong immunity and there is no degradation of tissue due to the growth of a tumor, then α_v=1, instead of $\alpha_v=1.3 \times 10^{-4}$ (as used in our entire estimation); the saturated tumor volume will be reduced by 7692 time for a particular f_{TS} and K_v. Hence, it is very difficult for a tumor to grow up to 1-2 mm^3 size when normal external tissue does not give space by degrading itself. From equations (3a) & (3e), it is observed that N_{TM} and V_{TM} of a tumor are inversely proportional to K_v, when other parameters remain unchanged. The result shows the possibility of minimizing tumor population and size by enhancing the elasticity of normal brain tissues. Again, a tumor has a lesser death rate, smaller $\alpha_{r,}$ and (when $\delta \neq 0$) has a larger value of N_{TM}, n_{TM}, A_{csM} and r_0. T_s and n_{TM} increase with α_{pn0} for a tumor.

Tumor angiogenesis plays an important role in tumor growth, invasion, and metastasis[42]. Angiogenesis and hyper-permeability of the tumor vessels are necessary for increased nutrient flux from capillaries to the interstitial space of a tumor to meet the greater demand for energy[22]. Hence, in histological sections, densities of microvessels and cells in brain tumors are found much higher than those of the normal tissue[19]. The rate of energy supplied per unit volume of tumor is given by the term $E_{su}=\alpha_{sr}\alpha_{s0}\alpha_{an}n_T$; which increases with the increase of n_T till the tumor is saturated. The energy consumption rate is more in high-grade brain tumors, though estimated α_{an} is found less in high grade than the low grade. The saturated cell density 'n_{TM}' of a tumor is higher if it maintains a larger rate of microvascular energy supply to each tumor cell. The parameter, α_{sr} increases with the hyper-permeability of the microvessels. Hence, high-grade tumor has to increase its α_{sr} to increase n_{TM}.

The growth rate in gliomas was investigated by many researchers using a tumor growth model considering the proliferation and migration of tumor cells[8,16,43-44]. The range of the growth rate reported by these workers was 1.70-50.29 yr^{-1}. In the present study, we have found that the growth rate falls from the initial maximum value 'r_0' to the minimum value at saturation 'r_s'. In the demonstration of our model, using reported data of gliomas, the estimated r_0 and r_s are found within the previously reported range.

Selection of proper value of the parameters α_{pn0}, α_v, α_{ps}, and α_{an} is very important for accurate estimation of saturated parameters n_{TM}, A_{csM}, N_{TM}, V_{TM}, T_s, and growth rate. The parameters K_v, $V_{T,}$ and total energy consumption rate of a tumor can be determined for a brain tumor by using advanced radiological diagnosis and PET scan. The histological diagnosis with n_T and A_{cs} evaluated by image morphometry of biopsy samples could be obtained for such tumors. Availability of experimentally obtained values could provide an accurate determination of the parameters used in this study. Again, in the actual scenario, when one parameter is modified, all other parameters of a tumor could be affected. The spatial growth pattern and tumor cell diffusion are not included in this model; which can be studied in the future for a better understanding of tumor proliferation and metastasis.

Conclusion

Using measured data of tumor cell density, microvessel size and density, tumor volume at different times, and overall energy consumptions by a tumor and elasticity of tissue, and integrating the information into an appropriate tumor growth model, one can predict the outcome of a tumor properly. The tumor saturation factor is an important feature to forecast the ultimate status of a tumor. Experimental investigation of cell and microvessel density in the early stage of a tumor is a challenging task; even we are not able to find any theoretical expression for the same. Using the present theoretical model, one can predict the temporal variation of tumor cell density, microvessel density, tumor cell population, size and growth rate; and their saturated values at different conditions. A tumor, having a larger microvascular supply of nutrients, lesser requirement of energy for maintenance, and smaller value of elastic modulus and resistance of normal tissue will attain

larger cell density and volume at saturation. Such information contributes to understanding tumor behavior in a better way and maybe exploited for the optimization of anti-cancer therapy.

Acknowledgement

The authors are grateful to The Director and Commandant, AFMC and DRDO for their support to perform the work.

Conflict of interest

All authors declare no conflicts of interest.

References

1 Jarrett AM, Lima EABF, Hormuth DA, McKenna MT, Feng X & Ekrut DA, Mathematical models of tumor cell proliferation: A review of the literature. *Expert Rev Anticancer Ther*, 18 (2018) 1271.

2 Enderling H & Chaplain MAJ, Mathematical modeling of tumor growth and treatment. *Curr Pharm Des*, 20 (2014) 4934.

3 Gao X, McDonald JT, Hlatky L & Enderling H, Acute and fractionated irradiation differentially modulate glioma stem cell division kinetics. *Cancer Res*, 73 (2013) 1481.

4 Boruah D, Effect of energy requirements in the growth of brain tumor: a theoretical approach. *Biomed Phys Eng Express*, 8 (2022) 015003.

5 Gandolfi A, Franciscis SD, D'Onofrio A, Fasano A & Sinisgalli C, Angiogenesis and vessel co-option in a mathematical model of diffusive tumor growth: the role of chemotaxis. *J Theoretical Biol*, 512 (2021) 110526.

6 Macklin P, Edgerton ME, Thompson AM & Cristini V, Patient calibrated agent-based modeling of ductal carcinoma *in situ* (DCIS): from microscopic measurements to macroscopic predictions of clinical progression. *J Theoretical Biol*, 301 (2012) 122.

7 Lesart AC, Sanden DVD, Hamard L, Estève F & Stéphanou A, On the importance of the submicrovascular network in a computational model of tumour growth. *Microvasc Res*, 84 (2012) 188.

8 Rockne R, Rockhill JK, Mrugala M, Spence AM, Kalet I, Hendrickson K, Lai A, Cloughesy T, Alvord-Jr EC & Swanson KR, Predicting the efficacy of radiotherapy in individual glioblastoma patients in vivo: a mathematical modeling approach. *Phys Med Biol*, 55 (2010) 3271.

9 Sturrock M, Miller IS, Kang G, Arba'ie NH, O'Farrell AC, Barat A, Marston G, Coletta PL, Byrne AT & Prehn JH, Anti-angiogenic drug scheduling optimization with application to colorectal cancer. *Sci Rep*, 8 (2018) 11182.

10 Powathil GG, Gordon KE, Hill LA & Chaplain MAJ, Modeling the effects of cell-cycle heterogeneity on the response of a solid tumour to chemotherapy. Biological insights from a hybrid multiscale cellular automaton model. *J Theoretical Biol*, 308 (2012) 1.

11 Jayatilaka H, Umanzor FG, Shah V, Meirson T, Russo G, Starich B, Tyle P, Lee JSH, Khatau S, Gil-Henn H & Wirtz D, Tumor cell density regulates matrix metalloproteinases for enhanced migration**.** *Oncotarget*, 9 (2018) 32556.

12 Von-Manstein V & Groner B, Tumor cell resistance against targeted therapeutics: the density of cultured glioma tumor cells enhances Stat3 activity and offers protection against the tyrosine kinase inhibitor canertinib. *Med Chem Commun*, 8 (2017) 96.

13 Clatz O, Sermesant M, Bondiau PY, Delingette H, Warfield SK, Malandain G & Ayache N, Realistic simulation of the 3-D growth of brain tumors in MR images coupling diffusion with biomechanical deformation. *IEEE Transactions on Medical Imaging*, 24 (2005) 1334.

14 Swanson KR, Rostomily RC & Alvord EC, A mathematical modelling tool for predicting survival of individual patients following resection of glioblastoma: A proof of principle. *Br J Cancer*, 98 (2008) 113.

15 Konukoglu E, Clatz O, Bondiau PY, Delingette H & Ayache N, Extrapolating glioma invasion margin in brain magnetic resonance images: Suggesting new irradiation margins. *Med Image Anal*, 14 (2010) 111.

16 Konukoglu E, Clatz O, Menze BJ, Stieltjes B, Weber MA, Mandonnet E & Delingette H, Ayache N, Image guided personalization of reaction-diffusion type tumor growth models using modified anisotropic eikonal equations. *IEEE Trans Med Imaging*, 29 (2010) 77.

17 De-Anta JM, Real FX & Mayol X, Low tumor cell density environment yields survival advantage of tumor cells exposed to MTX *in vitro*. *Biochim Biophys Acta*, 1721 (2005) 98.

18 Herholz K, Pietrzyk U, Voges J, Schroder R, Halber M, Treuer H, Strum V & Heiss WD, Correlation of glucose consumption and tumor cell density in astrocytomas: A stereotactic PET study. *J Neurosurg*, 79 (1993) 853.

19 Boruah D, Deb P, Srinivas V & Mani NS, Morphometric study of nuclei and microvessels in gliomas and its correlation with grades. *Microvasc Res*, 93 (2014) 52.

20 Boruah D & Deb P, Utility of nuclear morphometry in predicting grades of diffusely infiltrating gliomas. *ISRN Oncol*, (2013) 760653.

21 Deb P, Boruah D & Dutta V, Morphometric study of microvessels in primary CNS tumours and its correlation with tumour types and grade. *Microvasc Res*, 84 (2012) 34.

22 Carmeliet P & Jain RK, Angiogenesis in cancer and other diseases. *Nature*, 407 (2000) 249.

23 Kimberley MD & Vincent JMD, Normal organ weights in men. *Am J Forensic Med Pathol*, 33 (2012) 368.

24 Kimberley MD & Vincent JMD, Normal organ weights in women. *Am J Forensic Med Pathol*, 36 (2015) 182.

25 Elia M, Organ and tissue contribution to metabolic rate. *Energy metabolism: Tissue determinants and cellular corollaries*, (Kinney JM & Tucker HN, Raven Press, New York) 1992, 61.

26 Wang ZM, Ying Z, Bosy-Westphal A, Zhang J, Heller M, Later W, Heymsfield SB & Muller MJ, Evaluation of specific metabolic rates of major organs and tissues: Comparison between nonobese and obese women. *Obesity*, 20 (2012) 95.

27 Ganpule S, Daphalapurkar NP, Pirtini MC & Ramesh KT, Effect of bulk modulus on deformation of the brain under rotational accelerations. *Shock Waves*, 28 (2018) 127.

28 Jain RK, Martin JD & Stylianopoulos T, The role of mechanical forces in tumor growth and therapy. *Annu Rev Biomed Eng*, 16 (2014) 321.

29 Stylianopoulos T, Martin JD, Chauhan VP, Jain SR, Diop-Frimpong B, Bardeesy N, Smith BL, Ferrone CR, Hornicek FJ, Boucher Y, Munn LL & Jain RK, Causes, consequences, and remedies for growth-induced solid stress in murine and human tumors. *Proc Natl Acad Sci*, 109 (2012) 15101.

30 Albeck MJ, Borgesen SE, Gjerris F, Schmidt JF & Sorensen PS, Intracranial pressure and cerebrospinal fluid outflow conductance in healthy subject. *J Neurosurg*, 74 (1991) 597.

31 Nejad AE, Najafgholian S, Rostami A, Sistani A, Shojaeifar S, Esparvarinha M, Nedaeinia R, Javanmard SH, Taherian M, Ahmadlou M, Saheli R, Sadeghi B & Manian M, The role of hypoxia in the tumor microenvironment and development of cancer stem cell: a novel approach to developing treatment. *Cancer Cell Int*, 21 (2021) 62.

32 Krock BL, Skuli N & Simon MC, Hypoxia-induced angiogenesis: good and evil. *Genes & Cancer*, 2 (2011) 1117.

33 Zimna A & Kurpisz M, Hypoxia-inducible factor-1 in physiological and pathophysiological angiogenesis: applications and therapies. *BioMed Res Int*, (2015) 549412.

34 Marsters P, Alhamdan R & Campbell BK, Cell density-mediated pericellular hypoxia and the local dynamic regulation of VEGF-A splice variants in ovine ovarian granulosa cells division. *Biol Reprod*, 91 (2014) 35.

35 Behzadian MA, Wang Xi-L, Shabrawey M & Caldwell BR, Effects of hypoxia on glial cell expression of angiogenesis-regulating factors VEGF and TGF-b. *GLIA*, 24 (1998) 216.

36 Romero-Garcia S, Lopez-Gonzalez JS, Báez-Viveros JS, Aguilar-Cazares D & Prado-Garcia H, Tumor cell metabolism: An integral view. *Cancer Biol Ther*, 12 (2011) 939.

37 Hanahan D & Weinberg AE, Hallmarks of Cancer: The Next Generation. *Cell*, 144 (2011) 646.

38 Atuegwu NC, Gore JC & Yankeelov TE, The integration of quantitative multi-modality imaging data into mathematical models of tumors. *Phys Med Biol*, 55 (2010) 2429.

39 Guyon J, Chapouly C, Andrique L, Bikfalvi A & Daubon T, The normal and brain tumor vasculature: Morphological and functional characteristics and therapeutic targeting. *Front Physiol*, 12 (2021) 622615.

40 Chang YY, Wang LY, Liu CY, Chien TJ, Chen J & Hsu CH, The effects of a mindfulness meditation program on quality of life in cancer outpatients: An exploratory study. *Integr Cancer Ther*, 17 (2018) 363.

41 Budday S, Sommer G, Birkl C, Langkammer C, Haybaeck J, Kohnert J, Bauer M, Paulsen F, Steinmann P, Kuhl E & Holzapfel GA, Mechanical characterization of human brain tissue. *Acta Biomaterialia*, 48 (2017) 319.

42 Jiang X, Wang J, Deng X, Xiong F, Zhang S, Gong Z, Li X, Cao K, Deng H, He Y, Liao Q, Xiang B, Zhou M, Guo C, Zeng Z, Li G, Li X & Xiong W, The role of microenvironment in tumor angiogenesis. *J Exp Clin Cancer Res*, 39 (2020) 204.

43 Lipková J, Angelikopoulos P, Wu S, Alberts E, Wiestler B, Diehl C, Preibisch C, Pyka T, Combs SE, Hadjidoukas P, Leemput KV, Koumoutsakos P, Lowengrub J & Menze B, Personalized radiotherapy design for glioblastoma: Integrating mathematical tumor models, multimodal scans and bayesian inference. *IEEE Trans Med Imaging*, 38 (2019) 1875.

44 Rockne RC, Trister AD, Jacobs J, Hawkins-Daarud AJ, Neal ML, Hendrickson K, Mrugala MM, Rockhill JK, Kinahan P, Krohon KA & Swanson KR, A patient-specific computational model of hypoxia-modulated radiation resistance in glioblastoma using 18F-FMISO-PET. *J R Soc Interface*, 12 (2015) 20141174.